



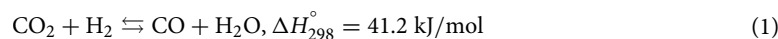
OPEN

Efficient reverse water gas shift reaction at low temperatures over an iron supported catalyst under an electric field

Masaki Yamaoka¹, Keidai Tomozawa¹, Koki Sumiyoshi¹, Tadaharu Ueda^{1,2,3} & Shuhei Ogo^{1,2}✉

The development of high-performance Fe-based catalysts is attractive because Fe is a cost-effective and earth-abundant element. Application of an external electric field and an appropriate catalytic support to an Fe-based catalyst enabled the reverse water–gas shift reaction to proceed with high activity, selectivity, and durability even at the low temperature of 423 K. The Fe-supported catalyst showed superior CO selectivity ($\approx 100\%$) compared to the Co- or Ni-supported catalyst. The apparent activation energy (5.9 kJ mol^{-1}) over the Fe/Ce_{0.4}Al_{0.1}Zr_{0.5}O₂ catalyst under an electric field was much lower than that without an electric field (61.4 kJ mol^{-1}).

Extensive attention has been given to solving the important issue that anthropogenic emissions of greenhouse gases such as CO₂ could accelerate global warming. Recently, a variety of CO₂ capture and utilization (CCU) technologies have been developed because they are regarded as effective ways to reduce artificial CO₂ emissions^{1–3}. Catalytic conversion of CO₂ with green H₂ produced by electrolysis of water using renewable energies is a promising candidate for CCU technology⁴. Many methods for converting CO₂ into valuable chemicals, such as CH₄, CO, and CH₃OH, have been reported^{4–12}. In particular, CO production from CO₂ through the reverse water–gas shift (RWGS) reaction (Eq. 1) is quite important because CO can be further converted into high-value chemicals and fuels, such as hydrocarbons and various oxygenates, via Fischer–Tropsch (FT) synthesis or well-established industrial processes, respectively^{4,13,14}, which is mainstream for C1 chemistry.



However, high-temperature heating is required to obtain high CO₂ conversion due to the thermodynamic equilibrium constraints for the RWGS reaction, leading to many problems in terms of energy and catalyst durability. Therefore, CO₂ conversion at low temperatures requires unconventional catalytic reaction techniques. In particular, the application of an external direct current electric field to metal-supported metal oxide semiconductor catalysts has enabled several catalytic reactions^{15,16} that include CO₂ activation, such as the RWGS reaction^{17,18}, CO₂ methanation⁵ and dry reforming of methane^{19,20}, to proceed even below 473 K. Both surface hydrogen migration and redox reactions that use lattice oxygen vacancies of metal oxide supports promoted by an electric field have resulted in the RWGS reaction proceeding smoothly and selectively with redox reactions even at low temperatures over Ru-supported catalysts¹⁸.

Highly active and selective catalysts for the RWGS reaction have been extensively developed²¹ based on various precious metal-supported materials (e.g., Pt/La–ZrO₂¹⁷, Rh/Fe–CeO₂²², Ru/ZrTiO₄¹⁸, PtMn/SiO₂²³) and base metal materials (e.g., Fe-based²⁴, Ni-based²⁵, Cu-based catalysts²⁶). Considering the amount and price of metal resources, Fe-based catalysts should be preferred for practical use. However, preparing stable high-performance Fe-based catalysts with high Fe dispersion is difficult because the supported Fe particles easily agglomerate during catalyst preparation, prereduction and/or catalytic reactions. On the other hand, the anchoring effect of Al doped in an oxide support effectively suppresses agglomeration of the supported Fe particles²⁷. Such highly dispersed Fe catalysts could exhibit high activity and stability in low-temperature RWGS reactions under an electric field. In this study, high-performance Fe-supported catalysts were developed by controlling the interaction between support oxides and supported Fe for use in the RWGS reaction under an electric field.

¹Department of Marine Resources Science, Faculty of Agriculture and Marine Science, Kochi University, Nankoku, Kochi 783-8502, Japan. ²Marine Core Research Institute, Kochi University, Nankoku, Kochi 783-8502, Japan. ³MEDI Center, Kochi University, Kochi 780-0842, Japan. ✉email: ogo@kochi-u.ac.jp

Results and discussion

Catalytic activity tests for the RWGS reaction under an electric field were conducted with 10 wt% Fe, Co, or Ni supported on $\text{Ce}_{0.4}\text{Al}_{0.1}\text{Zr}_{0.5}\text{O}_2$ (CAZO) to elucidate the effects of the supported metal on the catalytic activity and selectivity (Fig. 1). All of the tested M/CAZO catalysts showed catalytic activity even at the low temperature of 423 K. In particular, the Fe-supported catalyst exhibited higher CO selectivity (ca. 100%), although its catalytic activity was slightly lower, while the Co- and Ni-supported catalysts exhibited high CH_4 selectivity. The CO_2 conversion over the Fe- and Co-supported catalysts increased with increasing applied current, while that over the Ni-supported catalyst was independent of the applied current. Clearly, the supported metal affected the catalytic activity and selectivity, and the Fe-supported catalyst was suitable for obtaining CO from the RWGS reaction with high selectivity.

The catalytic activity was investigated by using the Fe-supported CAZO catalysts with various Fe loading amounts to clarify the effect of the Fe loading amount on the RWGS activity under an electric field at various input currents (Fig. 2). The CAZO support without Fe loading showed no catalytic activity. The CO_2 conversion increased with increasing Fe loading up to 10 wt% and then became constant. Although the number of active sites was sufficiently large at 10 wt% Fe, the activity increased proportional to the input current. The catalytic activity depends on both the Fe loading amount and the input current. Moreover, these Fe-supported catalysts under applied 1–5 mA currents exhibited nearly 100% CO selectivity (Fig. 2).

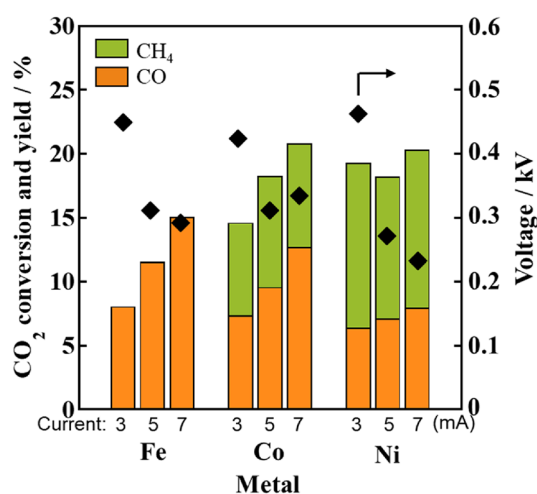


Figure 1. CO_2 conversion and product yields in the RWGS reaction over various 10 wt% metals supported on $\text{Ce}_{0.4}\text{Al}_{0.1}\text{Zr}_{0.5}\text{O}_2$ at 423 K under an electric field. Furnace temperature: 423 K; catalyst weight: 100 mg; input current (mA): 3.0, 5.0, and 7.0; gas composition (%): $\text{CO}_2:\text{H}_2:\text{Ar} = 25:25:50$; total gas flow rate: 100 mL min^{-1} .

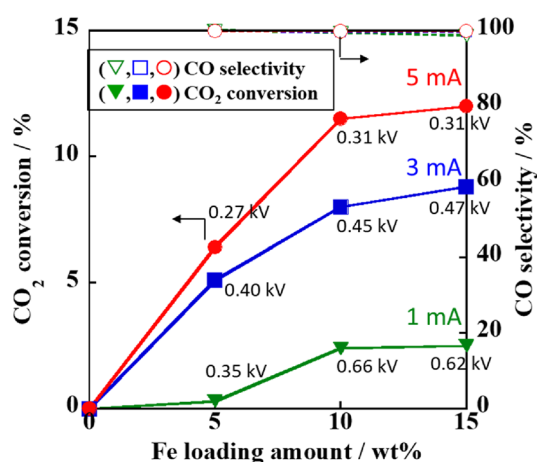


Figure 2. Effect of the Fe loading amount on the CO_2 conversion and CO selectivity in the RWGS reaction over the Fe/CAZO catalysts under an electric field at various input currents. Furnace temperature: 423 K; catalyst weight: 100 mg; input current (mA): (green filled triangles) 1.0, (blue filled squares) 3.0, and (red filled circles) 5.0; gas composition (%): $\text{CO}_2:\text{H}_2:\text{Ar} = 25:25:50$; total gas flow rate: 100 mL min^{-1} .

The catalytic activity was also investigated by using Fe-supported catalysts with different supports, such as CeO_2 , $\text{Ce}_{0.5}\text{Zr}_{0.5}\text{O}_2$ (CZO) or CAZO, to clarify the effect of the support on the catalytic RWGS activity under an electric field. All three Fe-supported catalysts under an applied 3–7 mA current exhibited nearly 100% CO selectivity (Fig. 3), and the highest CO_2 conversion was observed for the Fe/CAZO catalyst. The CO_2 conversion was correlated with the response voltage because of the galvanostatic control. The CO_2 conversion increased with the applied electric power (Fig. 3b), independent of the catalytic support, implying that the promoting effects of the electric field is almost the same for the three Fe-supported catalysts.

By applying Scherrer's equation, the crystallite sizes of the supported Fe were calculated to be $d = 27.5$, 36.7 and 27.5 for Fe/ CeO_2 , Fe/CZO, and Fe/CAZO, respectively, based on the X-ray diffraction (XRD) patterns of the three Fe-supported catalysts (Fig. S1). The catalytic activity was independent of the crystallite size, although the crystallite size of Fe/CZO was slightly larger than that of the other catalysts. The support affected the electronic and/or ionic conductivity rather than the particle size of the supported Fe, indicating that Fe/CAZO, for which a higher voltage (power) could be applied, exhibited higher catalytic activity.

The catalytic activity for the RWGS reaction was investigated at the designated catalyst bed temperature under different powers of the electric field generated by various applied currents (Fig. 4). The black line indicates the equilibrium conversion of the RWGS reaction at $\text{CO}_2:\text{H}_2 = 1:1$. Under an electric field, the CO_2 conversion

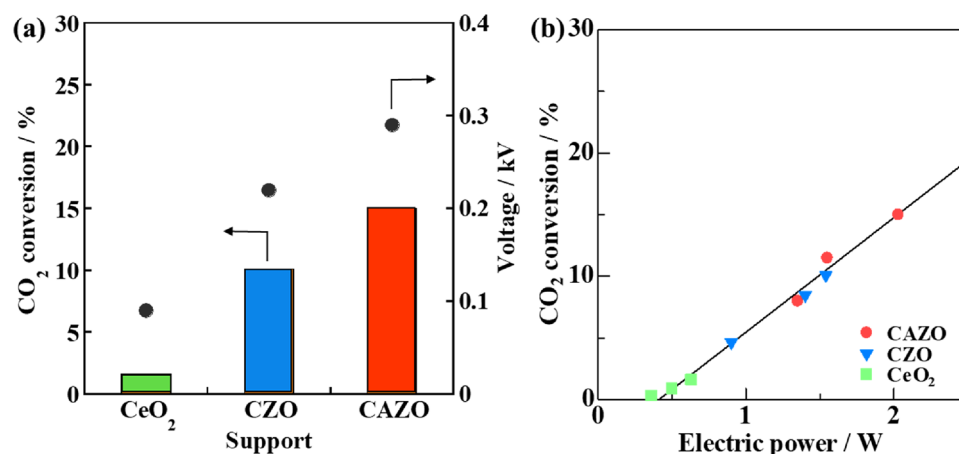


Figure 3. (a) Effects of the support on the CO_2 conversion and response voltage and (b) effect of the input electric power on the CO_2 conversion for the RWGS reaction over 10 wt% Fe-supported catalysts at 423 K under an electric field. Furnace temperature: 423 K; catalyst weight: 100 mg; input current (mA): 3.0–7.0; gas composition (%): $\text{CO}_2:\text{H}_2:\text{Ar} = 25:25:50$; total gas flow rate: 100 mL min^{-1} .

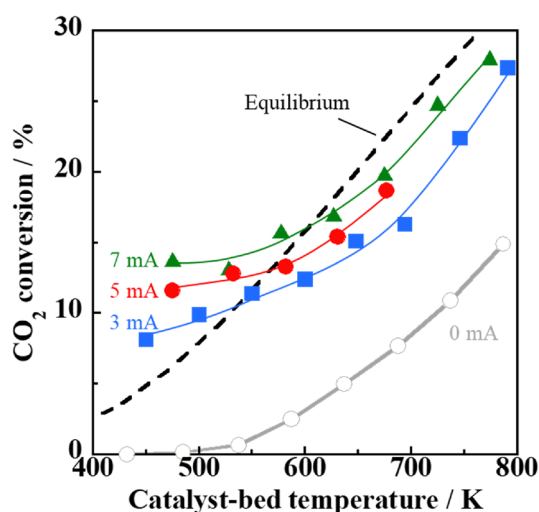


Figure 4. Temperature dependence of the CO_2 conversion in the RWGS reaction over the Fe/CAZO catalyst under an electric field with various applied currents. Furnace temperature: 423–773 K; catalyst weight: 100 mg; input current (mA): (grey unfilled circles) 0, (blue filled squares) 3, (red filled circles) 5, (green filled triangles) and 7; gas composition (%): $\text{CO}_2:\text{H}_2:\text{Ar} = 25:25:50$; total gas flow rate: 100 mL min^{-1} .

exceeded the equilibrium conversion in the low-temperature region below 550 K, while no catalytic activity was observed in the conventional RWGS reaction without an electric field (0 mA). The catalytic activity of the Fe/CAZO catalysts under an electric field below 550 K was comparable to that of the Ru-supported catalysts¹⁸. When a higher current was applied, more CO₂ was converted at the same catalyst bed temperature. The actual catalyst bed temperature, which was measured using a thermocouple, increased by 30–50 K due to Joule heating. The RWGS reaction proceeded even at low catalyst bed temperatures such as 475 K (423 K as the external temperature) when an electric field (5 mA) was applied, while no RWGS reaction proceeded at the same temperature without an electric field. Therefore, in the lower temperature region at approximately 500 K, Joule heating did not affect the catalytic activity under an electric field.

From the Arrhenius plots for the RWGS reaction over the Fe/CAZO catalyst (Fig. 5), the apparent activation energy was estimated to be $E_a = 5.9 \text{ kJ mol}^{-1}$ under an electric field, which was much lower than the value of $E_a = 61.4 \text{ kJ mol}^{-1}$ without an electric field. The difference in the apparent activation energy indicates that the reaction mechanism of the RWGS reaction under an electric field should be different from that of the conventional catalytic RWGS reaction without an electric field. Recently, the RWGS reaction over a Ru/ZrTiO₄ catalyst under an electric field ($E_a = 6.74 \text{ kJ mol}^{-1}$) was reported to proceed through a redox mechanism based on in situ diffuse reflectance infrared Fourier transform spectroscopy measurements, in which the electric field promoted the formation of lattice oxygen vacancies on the surface of the metal oxide support to reduce CO₂ to CO using the formed surface lattice oxygen vacancies even at low temperatures¹⁸. A periodic operation test was conducted on the Fe/CAZO catalyst under an electric field at 423 K (see the Supporting Information), and the results also supported this redox reaction mechanism. The observation that CO was produced when CO₂ was supplied but not when H₂ was supplied (Fig. S2) indicates that the RWGS reaction over the Fe/CAZO catalyst under an electric field could proceed through a redox mechanism similar to that for the reported Ru/ZrTiO₄ catalyst system. Moreover, the observation that the amount of CO formed during CO₂ supply without an electric field was significantly reduced (Fig. S3) indicates that an electric field must promote the redox reaction involving lattice oxygen vacancies.

The CO₂ conversion and CO selectivity variations with time on stream were investigated to evaluate the catalytic stability of the Fe/CAZO catalyst under an electric field (Fig. 6 and Fig. S4). The CO₂ conversion remained constant at approximately 10%, despite some fluctuations, with the CO selectivity remaining constant at 100% for at least 8 h, indicating that the Fe/CAZO catalyst should be highly stable with high activity and selectivity for the RWGS reaction under an electric field.

Conclusions

The catalytic performance of Fe-supported catalysts, i.e., Fe/CeO₂, Fe/Ce_{0.5}Zr_{0.5}O₂ (Fe/CZO) and Fe/Ce_{0.4}Al_{0.1}Zr_{0.5}O₂ (Fe/CAZO), was investigated for the RWGS reaction with and without an electric field at 423 K. Fe/CAZO exhibited high CO₂ conversion and CO selectivity (ca. 100%), with its catalytic performance being maintained for at least 8 h. The apparent activation energy was estimated to be 5.9 kJ mol^{-1} under an electric field, which was much lower than that without an electric field (61.4 kJ mol^{-1}). The application of an electric field to catalysts enables low-temperature selective CO₂ conversion to proceed even though no activity was observed

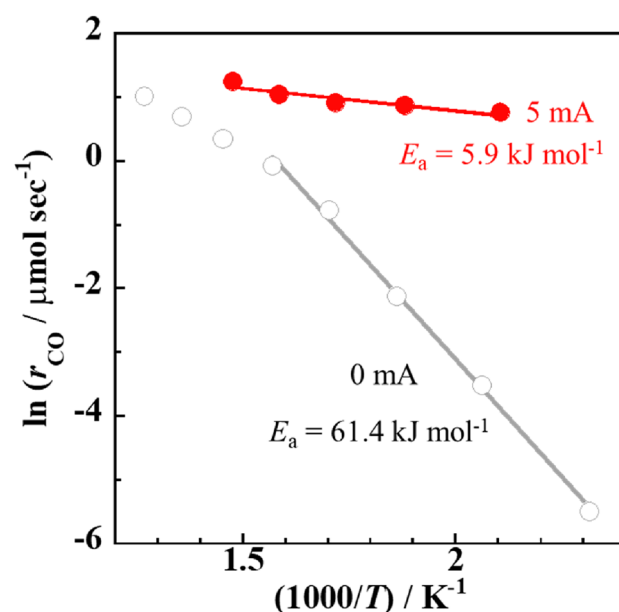


Figure 5. Arrhenius plots for the RWGS reaction over the Fe/CAZO catalyst with or without an electric field. Furnace temperature: 423–773 K; catalyst weight: 100 mg; input current (mA): (grey unfilled circles) 0 and (red filled circles) 5; gas composition (%): CO₂:H₂:Ar = 25:25:50; total gas flow rate: 100 mL min⁻¹.

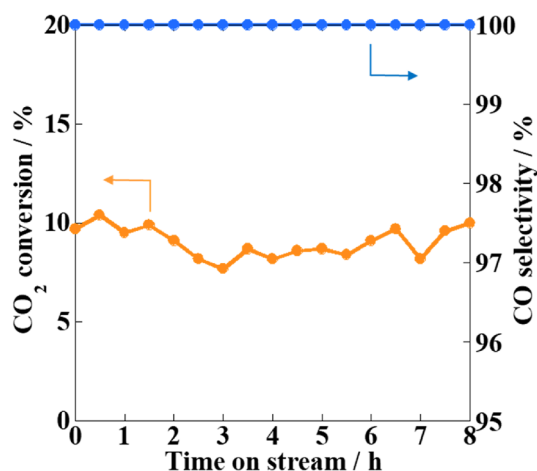


Figure 6. Catalytic stability during the RWGS reaction over the Fe/CAZO catalyst under an electric field. Furnace temperature: 423 K; catalyst weight: 100 mg; input current: 5.0 mA; gas composition (%): CO₂:H₂:Ar = 25:25:50; total gas flow rate: 100 mL min⁻¹.

in the conventional RWGS reaction without an electric field (0 mA). This is the first report showing that the RWGS reaction proceeds over Fe-based catalysts without platinum group metals (PGM) at low temperatures below 500 K. These results will lead to the creation of a new CO₂ recycling technology that uses an inexpensive/abundant Fe-based catalyst and unused low-temperature waste heat.

Experimental

Catalyst preparation

CeO₂ was supplied by the Catalyst Society of Japan (JRC-CEO-1). Ce_{0.5}Zr_{0.5}O₂ (denoted as CZO) and Ce_{0.4}Al_{0.1}Zr_{0.5}O₂ (denoted as CAZO) were prepared using a complex polymerization method based on a synthetic procedure presented in the literature as follows²⁷. Citric acid monohydrate (FUJIFILM Wako Pure Chemical Co.) and ethylene glycol (FUJIFILM Wako Pure Chemical Co.) were dissolved in 200 mL of distilled water and stirred. Then, stoichiometric amounts of Ce(NO₃)₃·6H₂O (FUJIFILM Wako Pure Chemical Co.), ZrO(NO₃)₂·2H₂O (FUJIFILM Wako Pure Chemical Co.) and Al(NO₃)₃·9H₂O (FUJIFILM Wako Pure Chemical Co.) were added to the solution and stirred. The molar ratios of metal, citric acid monohydrate and ethylene glycol were 1:3:3. The prepared solution was heated on a hot plate at 523 K with stirring to remove water and then dried in an oven at 343 K overnight. The obtained powder was calcined at 773 K for 5 h (5 K min⁻¹).

Using Fe(NO₃)₃·9H₂O (FUJIFILM Wako Pure Chemical Co.), Co(NO₃)₂·6H₂O (FUJIFILM Wako Pure Chemical Co.) or Ni(NO₃)₂·6H₂O (FUJIFILM Wako Pure Chemical Co.) as precursors, 10 wt% Fe, Co or Ni, respectively, was supported on the prepared supports by an impregnation method based on a synthetic procedure presented in the literature as follows²⁸. Each of the support powders was dispersed in 20 mL of distilled water and stirred for 2 h at room temperature *in vacuo*. Then, 20 mL of an aqueous solution of the metal precursor was added to the support-powder-dispersed solution and stirred for 2 h. The mixed solution was heated on a hot plate at 523 K with stirring to remove water and then dried in an oven at 343 K overnight. The obtained powder was calcined at 773 K for 2 h (5 K min⁻¹).

The crystalline structure of the prepared catalysts was characterized by powder X-ray diffraction (XRD; X'pert-PRO; PANalytical), which was performed at 45 kV and 40 mA using Cu-K α radiation. Diffractograms were taken at 2 θ angles of 3–75° with a step size of 0.01°.

Activity test

Catalytic activity tests with or without an electric field were conducted using a fixed-bed flow-type reactor with a quartz tube (6.0 mm i.d.), as shown in Fig. 7. The catalysts were sieved to 250–500 μ m, and 100 mg of each sample was charged into a reaction tube. For pretreatment, the catalyst was reduced at 773 K for 2 h under a H₂/Ar gas flow (H₂:Ar = 1:2, 75 mL min⁻¹). After the reduction, the furnace temperature was lowered to 423 K. The composition of the reactant feed gas was CO₂:H₂:Ar = 1:1:2 (100 mL min⁻¹). Two stainless-steel electrodes (2.0 mm o.d.) were inserted into each end of the catalyst bed to apply a direct current using a DC power supply. The catalyst bed temperature was directly measured using a thermocouple, which was inserted into the bottom side of the catalyst bed. After removal of the produced water using a cooling trap, product gases, including CO₂, CO, and CH₄, were analyzed using a gas chromatograph-flame ionization detector (GC-FID, GC-2014; Shimadzu Corp.) equipped with a Porapak Q packed column and a methanizer (MTN-1; Shimadzu Corp.). The CO₂ conversion and CO selectivity were calculated by the following equations (Eqs. 2 and 3, respectively):

$$\text{CO}_2 \text{ conversion (\%)} = (F_{\text{CO}_2,\text{out}} + F_{\text{CH}_4,\text{out}}) / F_{\text{CO}_2,\text{in}} \times 100 \quad (2)$$

$$\text{CO selectivity (\%)} = F_{\text{CO},\text{out}} / (F_{\text{CO},\text{out}} + F_{\text{CH}_4,\text{out}}) \times 100 \quad (3)$$

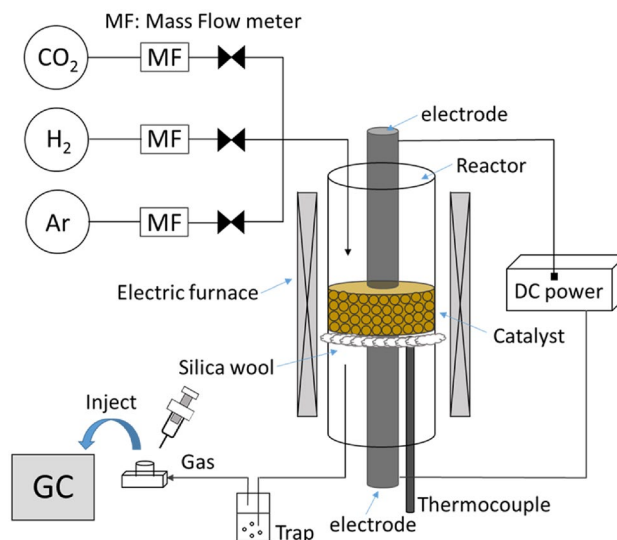


Figure 7. Schematic diagram of the reaction apparatus.

Data availability

Data is provided within the manuscript or supplementary information files.

Received: 27 February 2024; Accepted: 30 April 2024

Published online: 03 May 2024

References

- Cox, P. M., Betts, R. A., Jones, C. D., Spell, S. A. & Totterdell, I. J. Acceleration of global warming due to carbon-cycle feedbacks in a coupled climate model. *Nature* **408**, 184–187 (2000).
- Rogelj, J. *et al.* Paris Agreement climate proposals needs a boost to keep warming well below 2 °C. *Nature* **534**, 631–639 (2016).
- Davis, S. J., Caldeira, K. & Matthews, H. D. Future CO₂ emissions and climate change from existing energy infrastructure. *Science* **329**, 1330–1333 (2010).
- Tsubaki, N., Wang, Y., Yang, G. & He, Y. Rational design of novel reaction pathways and tailor-made catalysts for value-added chemicals synthesis from CO₂ hydrogenation. *Bull. Chem. Soc. Jpn.* **96**, 291–302 (2023).
- Yamada, K., Ogo, S., Yamano, R., Higo, T. & Sekine, Y. Low-temperature conversion of carbon dioxide to methane in an electric field. *Chem. Lett.* **49**, 303–306 (2020).
- Kwak, J. H., Kovarik, L. & Szanyi, J. Heterogeneous catalysis on atomically dispersed supported metal: CO₂ reduction on multifunctional Pd catalysts. *ACS Catal.* **3**, 2094–2100 (2013).
- Zhu, J. *et al.* Deconvolution of the particle size effect on CO₂ hydrogenation over iron-based catalysts. *ACS Catal.* **10**, 7424–7433 (2020).
- Liu, H.-X. *et al.* Partially sintered copper-ceria as excellent catalyst for the high-temperature reverse water gas shift reaction. *Nat. Commun.* **13**, 867 (2022).
- Zhu, Y. *et al.* Copper-zirconia interfaces in UiO-66 enable selective catalytic hydrogenation of CO₂ to methanol. *Nat. Commun.* **11**, 5849 (2020).
- Lam, E. *et al.* Isolated Zr surface sites on silica promote hydrogenation of CO₂ to CH₃OH in supported Cu catalysts. *Chem. Soc.* **140**, 10530–10535 (2018).
- Ting, K. W., Toyao, T., Siddiki, S. M. A. H. & Shimizu, K. Low-temperature hydrogenation of CO₂ to methanol over heterogeneous TiO₂-supported Re catalysts. *ACS Catal.* **9**, 3685–3693 (2019).
- Zhu, J. *et al.* Flame synthesis of Cu/ZnO-CeO₂ catalysts: Synergistic metal-support interactions promote CH₃OH selectivity in CO₂ hydrogenation. *ACS Catal.* **11**, 4880–4892 (2021).
- Xu, M., Cao, C. & Xu, J. Understanding kinetically interplaying reverse water-gas shift and Fischer-Tropsch synthesis during CO₂ hydrogenation over Fe-based catalysts. *Appl. Catal. A* **641**, 118682 (2022).
- Li, J. *et al.* Integrated tunable synthesis of liquid fuels via Fischer-Tropsch technology. *Nat. Catal.* **1**, 787–793 (2018).
- Ogo, S. & Sekine, Y. Catalytic reaction assisted by plasma or electric field. *Chem. Rec.* **17**, 1–14 (2017).
- Torimoto, M., Murakami, K. & Sekine, Y. Low-temperature heterogeneous catalytic reaction by surface protonics. *Bull. Chem. Soc. Jpn.* **92**, 1785–1792 (2019).
- Oshima, K. *et al.* Low temperature catalytic reverse water gas shift reaction assisted by an electric field. *Catal. Today* **232**, 27–32 (2014).
- Yamano, R., Ogo, S., Nakano, N., Higo, T. & Sekine, Y. Non-conventional low-temperature reverse water-gas shift reaction over highly dispersed Ru catalyst in an electric field. *EES Catal.* **1**, 125–133 (2023).
- Motomura, A. *et al.* Synergistic effects of Ni-Fe alloy catalysts on dry reforming of methane at low temperatures in electric field. *RSC Adv.* **12**, 28359–28363 (2022).
- Nakano, N. *et al.* Elucidation of the reaction mechanism on dry reforming of methane in an electric field by in-situ DRIFTS. *RSC Adv.* **12**, 9036–9043 (2022).
- Dazza, Y. A. & Kuhn, J. N. CO₂ conversion by reverse water gas shift catalysis: comparison of catalysts, mechanisms and their consequences for CO₂ conversion to liquid fuels. *RSC Adv.* **6**, 49675–49691 (2016).
- Kim, G. *et al.* Gas-permeable iron-doped ceria shell on Rh nanoparticles with high activity and durability. *JACS Au* **2**, 1115–1122 (2022).
- Liu, Y. *et al.* Promoting n-butane dehydrogenation over PtMn/SiO₂ through structural evolution induced by a reverse water-gas shift reaction. *ACS Catal.* **12**, 13506–13512 (2022).

24. Gu, M. *et al.* Structure-activity relationships of copper-and potassium-modified iron oxide catalysts during reverse water-gas shift reaction. *ACS Catal.* **11**(20), 12609–12619 (2021).
25. Alvarez-Galvan, C. *et al.* Highly active and stable Ni/La-doped ceria material for catalytic CO₂ reduction by reverse water-gas shift reaction. *ACS Appl. Mater. Interfaces* **14**(45), 50739–50750 (2022).
26. Zhang, X. *et al.* Highly dispersed copper over β -Mo₂C as an efficient and stable catalyst for the reverse water gas shift (RWGS) reaction. *ACS Catal.* **7**(1), 912–918 (2016).
27. Sakai, R. *et al.* Agglomeration suppression of a Fe-Supported catalyst and its utilization for low-temperature ammonia synthesis in an electric field. *ACS Omega* **5**, 6846–6851 (2020).
28. Torimoto, M. *et al.* Enhanced methane activation on diluted metal–metal ensembles under an electric field: breakthrough in alloy catalysis. *Chem. Commun.* **55**, 6693–6695 (2019).

Acknowledgements

This paper is based on results obtained from the NEDO Feasibility Study Program (Uncharted Territory Challenge 2050; 20M1E05Y).

Author contributions

M.Y. and S.O. designed the experiments, analyzed the data, and wrote the manuscript. M.Y., K.T., and K.S. conducted the experiments. T.U. supervised the project and revised the manuscript text. All authors reviewed the manuscript.

Competing interests

The authors declare no competing interests.

Additional information

Supplementary Information The online version contains supplementary material available at <https://doi.org/10.1038/s41598-024-61017-2>.

Correspondence and requests for materials should be addressed to S.O.

Reprints and permissions information is available at www.nature.com/reprints.

Publisher's note Springer Nature remains neutral with regard to jurisdictional claims in published maps and institutional affiliations.



Open Access This article is licensed under a Creative Commons Attribution 4.0 International License, which permits use, sharing, adaptation, distribution and reproduction in any medium or format, as long as you give appropriate credit to the original author(s) and the source, provide a link to the Creative Commons licence, and indicate if changes were made. The images or other third party material in this article are included in the article's Creative Commons licence, unless indicated otherwise in a credit line to the material. If material is not included in the article's Creative Commons licence and your intended use is not permitted by statutory regulation or exceeds the permitted use, you will need to obtain permission directly from the copyright holder. To view a copy of this licence, visit <http://creativecommons.org/licenses/by/4.0/>.

© The Author(s) 2024